Synchronous patterns in complex systems

Chenbo Fu,[1] Hong Zhang,[1,2] Meng Zhan,[3] and Xingang Wang[1,*]
[1]*Department of Physics, Zhejiang University, Hangzhou 310027, China*
[2]*Zhejiang Institute of Modern Physics, Hangzhou 310027, China*
[3]*Wuhan Institute of Physics and Mathematics, Chinese Academy of Sciences, Wuhan 430071, China*
(Received 6 April 2012; published 25 June 2012)

When a complex network is slightly desynchronized, a few of the network nodes will be escaping from the uniform synchronization background frequently with a random fashion, leading to the intermittent network synchronization. Here, based on the eigenvectors of the network coupling matrix, we propose a new method which is able to figure out the unstable nodes in the general case of desynchronized complex networks. Moreover, with this method, we are also able to regulate the seemingly random network dynamics into *stable and visible synchronous patterns*. The efficiency of this method is verified by a variety of network models, including varying the network structures, the node local dynamics, and the desynchronization types. Our studies show that, even for the complex network systems, synchronous patterns can still be identified and characterized.

DOI: 10.1103/PhysRevE.85.066208 PACS number(s): 05.45.Xt, 89.75.Hc

I. INTRODUCTION

An amazing feature of the spatiotemporal nonlinear systems in nature is that under certain conditions they can be self-organized into various patterns, which has stimulated the extensive studies of pattern formation over the past half century [1,2]. In general, the systems considered are homogeneous in space and the generated patterns are of regular structures, e.g., the Turing patterns in autocatalytic chemical reactions [3,4]. Recently, inspired by the rapid progress of network science, attentions have been also paid to the formation of patterns in inhomogeneous systems represented by complex networks [5–7]. However, due to the complexity of the network structure, the patterns in such systems are highly fragmented and scattered, making it difficult to be figured out [8,9]. Regarding this, one important issue in studying patterns in complex systems has been developing new methods for the purpose of pattern identification [10–12]. In Ref. [10], based on the properties of the critical mode characterzing the system destabilization, the authors have investigated the formation of Turing patterns in the network-organized activator-inhibitor systems, where some striking difference from the classical systems have been revealed. In Refs. [11,12], by a new method called dominant phase advanced driving (DPAD), the authors have successfully figured out the target-wave-like patterns in oscillatory complex networks consisting of a large number of excitable nodes, which gives a strong indication to the generation of rhythm clocks in many biological systems [13]. Despite of the progresses have been made, the study of pattern formation in complex network systems is still in its infancy, and many new forms of patterns are to be explored.

As a typical phenomenon of coupled oscillator systems, the synchronization behavior has attracted continuous interest in the field of nonlinear science [14,15]. Recently, initiated by the discovery of the small-world and scale-free properties in many real and man-made systems, a new surge of studies has been formed on the synchronization of complex networks [16,17], in which the important roles of the network topology on synchronization have been discovered [18,19]. Most of the studies, however, focus on only the stability of the homogeneous synchronization state, e.g., the global network synchronization, while the dynamics and stabilities of the inhomogeneous synchronization states have been largely overlooked, e.g., the synchronous patterns [20,21]. As global synchronization sometimes is regarded as harmful to the functioning of realistic systems, e.g., the epileptic seizure [22], the study of network desynchronization therefore is necessary and meaningful. The desynchronization of random networks has been investigated in Ref. [20], where an interesting finding is that, nearby the synchronization transition point, the network undergoes the typical process of on-off intermittency. Specifically, during the process of system evolution, a few of the network nodes are found to be escaping and rejoining the uniform synchronization background frequently with a random fashion. This small number of unstable nodes, while playing a key role in the network synchronization, have not yet been well characterized. For instance, it remains unknown *how to figure out the unstable nodes from the given network structure*.

In the present work, by the method of eigenvector analysis, we will show that the unstable nodes in the desynchronized complex systems indeed can be identified. A striking finding is that, after a reordering of the network nodes, the seemingly random dynamics of the desynchronized system can be transformed into *stable and visible synchronous patterns*. That is, the patterns familiar in the classical systems can still be observed in complex systems, but from a different viewpoint. The rest of the paper is organized as follows. In Sec. II, we shall present the model of complex network, and demonstrating the phenomenon of intermittent synchronization. In Sec. III, we shall first propose our new method for the identification of unstable nodes, and then showing how to figure out the synchronous patterns from the seemingly random dynamics. Pattern identification in clustered complex networks will be discussed in Sec. IV, in which the important roles of the network structures on patterns shall be addressed. Finally, in Sec. V we shall give our discussions and conclusion.

*Corresponding author: wangxg@zju.edu.cn

II. MODEL AND PHENOMENON

We consider the following model for the complex network of coupled nonlinear oscillators [19,23],

$$\dot{\mathbf{x}}_i = \mathbf{F}(\mathbf{x}_i) + \varepsilon \sum_{j=1}^{N} c_{ij}[\mathbf{H}(\mathbf{x}_j) - \mathbf{H}(\mathbf{x}_i)], \tag{1}$$

where $i,j = 1,\ldots,N$ are the node indices, $\mathbf{x}$ is a d-dimensional vector characterizing the oscillator (node) state, and ε is the uniform coupling strength. $\mathbf{F}$ and $\mathbf{H}$ represent, respectively, the dynamics of the isolated oscillators and the coupling function between them. The coupling matrix, C, is defined as $c_{ij} = a_{ij}/k_i$, where $\{a_{ij}\}$ is the adjacency matrix describing the network structure: $a_{ij} = 1$ if nodes i and j are directly connected in the network, and $a_{ij} = 0$ otherwise; and $k_i = \sum_j a_{ij}$ is the number of connections (degree) for the ith node. For simplicity, we employ the chaotic logistic map, $F(x) = 4x(1-x)$, as the node local dynamics, and using $H(x) = F(x)$ as the coupling function. (The findings established on this model are general for the complex network of coupled nonlinear oscillators, as will be discussed later.)

The synchronization of the above network can be analyzed by the method of master-stability-function (MSF) [24–26], which can be briefed as follows. Let x_s be the synchronous manifold of the oscillators and $\delta x_i = x_i - x_s$ be an infinitesimal distance that the ith oscillator is perturbed from x_s, then the evolution of δx_i is governed by the equation (in the linearized form)

$$\delta\dot{x}_i = \mathbf{DF}(x_s) + \varepsilon \sum_{j=1}^{N} c_{ij}\mathbf{DH}(x_s)(\delta x_j - \delta x_i), \tag{2}$$

where $\mathbf{DF}$ and $\mathbf{DH}$ are the Jacobian matrices of the corresponding vector functions evaluated on x_s. Projecting $\{\delta x_i\}$ into the eigenspace spanned by the eigenvectors, $\{\mathbf{e}_i\}$, of the coupling matrix $\mathbf{C}$, the set of equations described by Eq. (2) can be diagonalized into N decoupled mode equations

$$\delta\dot{y}_i = [\mathbf{DF}(x_s) + \varepsilon\lambda_i\mathbf{DH}(x_s)]\delta y_i, \tag{3}$$

where $0 = \lambda_1 > \lambda_2 \geqslant \cdots \geqslant \lambda_N$ are the eigenvalues of the coupling matrix and δy_i is the ith eigenmode associated with λ_i. Here, the two non-zero extreme eigenvalues, λ_2 and λ_N, are named the boundary eigenvalues. Denoting Λ_i as the largest Lyapunov exponent for the equation of mode i [calculated from Eq. (3) by λ_i], then, to make the network synchronizable, the necessary condition is that except the trivial mode δy_1 (which represents the motion of the synchronous manifold itself), all other modes of the system, $\{\delta y_l, l = 2,\ldots,N\}$, should be damping with time, i.e., $\Lambda(\sigma_l \equiv -\varepsilon\lambda_l) < 0$ for $l > 1$. Previous studies of MSF have shown that for the typical nonlinear oscillators, the value of Λ is only negative within a bounded region in the parameter space, $\sigma \in (\sigma_1,\sigma_2)$ [27]. For the specific case of chaotic logistic map considered here, we have $\sigma_1 = 0.5$ and $\sigma_2 = 1.5$ [21]. Therefore, to make the network synchronizable, the following two conditions, $-\varepsilon\lambda_2 > \sigma_1$ and $-\varepsilon\lambda_N < \sigma_2$, should be satisfied simultaneously. For the fixed network structure, if the eigenratio $R \equiv \lambda_N/\lambda_2 < \sigma_2/\sigma_1$, then whether the network can be synchronized is determined by solely the coupling strength, ε. Speaking alternatively, the network is only synchronizable in the regime $\varepsilon \in (\varepsilon_1,\varepsilon_2)$, with $\varepsilon_1 = -\sigma_1/\lambda_2$ and $\varepsilon_2 = -\sigma_1/\lambda_N$ the two critical points that mark the transitions of the network synchronization (which are also known as the long- and short-wave bifurcation points in previous studies of coupled regular networks [28,29]).

We start by showing the intermittency phenomenon of network synchronization around the above transition points. To simulate, we generate a scale-free-type network by the BA growth algorithm [6], which contains $N = 800$ nodes and the average node degree is $\langle k\rangle = 16$ [Fig. 1(a)]. From the network structure we can construct the coupling matrix, and then calculate the two boundary eigenvalues. For this specific network, we have $\lambda_2 \approx -0.53$ and $\lambda_N \approx -1.47$. By the MSF analysis briefed above, we can obtain the two transition points for the network synchronization, $\varepsilon_1 \approx 0.94$ and $\varepsilon_2 \approx 1.02$. In simulations, we first set the coupling strength to be inside the stable regime, $\varepsilon = 1$. Then, after the network is synchronized, we change the coupling strength to $\varepsilon = 0.935$, which is slightly below the transition point ε_1. In the meantime, the independent and identically distributed (iid) random noise with the strength $D = 1 \times 10^{-2}$ is added to the trajectories of the oscillators, so as to perturb the system from the synchronous state. It should be emphasized that, by this setting, only the 2nd eigenmode of the system is unstable, $\Lambda_1 \approx 6 \times 10^{-3}$, while the other eigenmodes are still in the stable regime, $\Lambda_l < 0, l = 2,\ldots,N$. The synchronization degree of the ith node to the whole network is evaluated by the error $\delta x_i' = |x_i - \bar{x}|$, with $\bar{x} = \sum_j x_j/N$ the network-averaged state. For the case of slightly desynchronized system, we roughly have $\bar{x} \approx x_s$, especially when the size of the network is large enough [24].

A snapshot of the synchronization errors is plotted in Fig. 1(a), where the value of $\delta x'$ is characterized by the size of the node. It is seen in this figure that the synchronization errors of a few of the network nodes are *distinguishingly* larger than the others. Besides the feature of heterogenous distribution, the synchronization errors are also timely varying. That is, the picture shown in Fig. 1(a) is non-stationary, and is changing with time. The dynamic feature of the synchronization errors is more clearly presented in Fig. 1(b), where $\delta x'$ is plotted as a function of time for all the network nodes. A phenomenon observed in Fig. 1(b) is that, during the system evolution, there are time intervals during which the whole network is highly synchronized, e.g., the episode from $t = 580$ to 600, as well as short periods where the network is seriously desynchronized, e.g., the time from $t = 800$ to 1.2×10^3. To characterize the evolution of the global network synchronization, we plot in Fig. 1(c) the network-averaged synchronization error, $\delta x'_{\rm net}(t) = \sum_{j=1}^{N} \delta x'_j(t)/N$ as a function of time. It is seen that as time increases, the value of $\delta x'_{\rm net}$ is frequently approaching 0 (reflecting a frequent visit of the oscillator trajectories to the synchronous manifold), as well as large bursts (showing the desynchronization of the network). This phenomenon, which is known as the on-off intermittency in traditional nonlinear studies [30,31], is general for the case of slightly desynchronized complex networks. (In Ref. [20], by a mean-field treatment, the problem of network synchronization is transformed to the stability analysis of a low-dimensional random dynamics, with which the on-off intermittency can be justified mathematically).

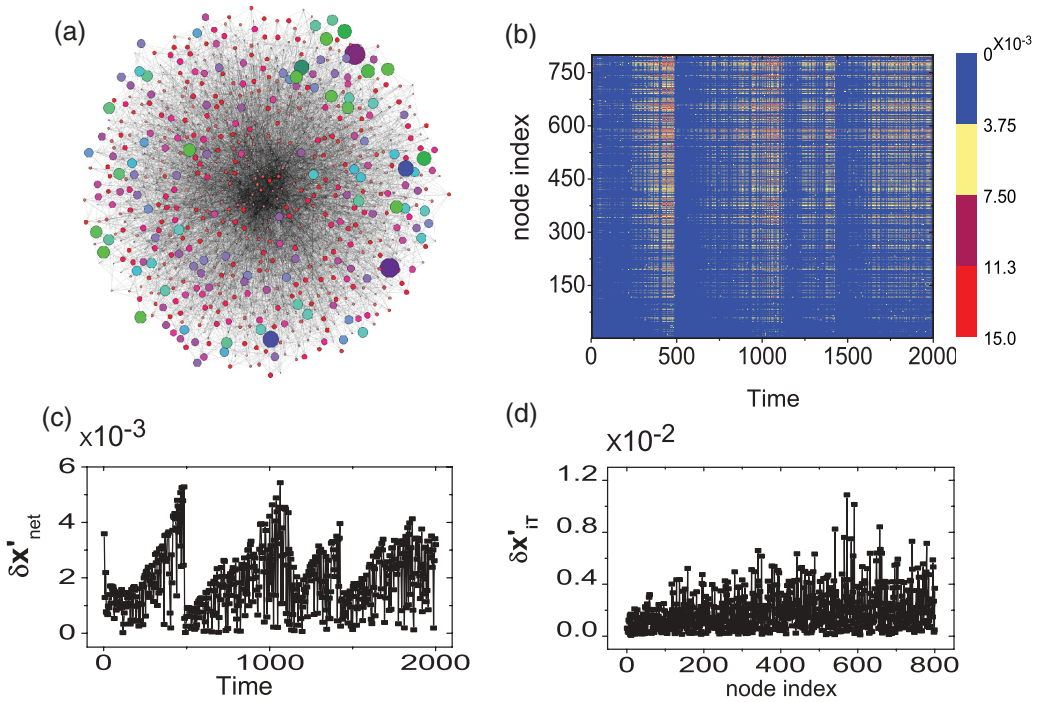

FIG. 1. (Color online) The intermittent synchronization of the networked chaotic logistic maps. The network is generated according to the BA growth algorithm, which contains $N = 800$ nodes and the average degree is 14. The uniform coupling strength is $\varepsilon = 0.935$, with which only the 2nd mode is slightly destabilized, $\Lambda_1 \approx 6 \times 10^{-3} > 0$. (a) A snapshot of the synchronization errors, $\delta x'_i$, where the size of the nodes is set to be proportional to the amplitude of the synchronization error, while the colors are used for eye guiding. (b) After a transient period of $t = 1 \times 10^3$, the time evolution of the synchronization errors, $\delta x'$, for all the network nodes. (c) The variation of the network-averaged synchronization error, $\delta x'_{\text{net}}$, as a function of time, which experiences the process of on-off intermittency. (d) The distribution of the time-averaged synchronization error, $\delta x'_{iT}$, where each data is averaged over a period of $T = 1 \times 10^3$. Our tasks in the present work are just to figure the unstable nodes in the complex network of (a), and identify the synchronous patterns in the seemingly random dynamics of (b).

Another interesting phenomenon observed in Fig. 1(b) is that, although of the timely intermittent evolution, the locations of the unstable nodes in the network are relatively stable. This can be partially seen from the interrupted horizontal lines in the figure. To quantify the synchronization stability of the individual nodes, we calculate the time-averaged synchronization error of the nodes, $\delta x'_{iT} = \sum_{t=1}^{T} \delta x'_i / T$, and plot the distribution in Fig. 1(d). Indeed, it is seen that for a few of the nodes the values of $\delta x'_T$ are distinguishingly large. In particular, the value of $\delta x'_T$ for the node 570 (the most unstable node) is larger than that of the node 11 (one of the most stable nodes) by about three orders. Our specific tasks of the present work therefore are: (1) figuring out the unstable nodes in the network structure of Fig. 1(a), and (2) identifying the synchronous pattern in the network dynamics of Fig. 1(b).

III. IDENTIFICATION OF UNSTABLE NODES AND SYNCHRONOUS PATTERNS

The locations of the unstable nodes can be predicted from the eigenvector of the destabilized mode in the network, with the details the following. Let $\mathbf{Q}$ be a $N \times N$ matrix whose ith column is composed by the ith normalized eigenvector of the coupling matrix (associated with the eigenvalue λ_i), we then have the following relationship between the trajectory perturbations, $\delta\mathbf{x} = (\delta x_1, \delta x_2, \ldots, \delta x_N)^T$, are the mode perturbations, $\delta\mathbf{y} = (\delta y_1, \delta y_2, \ldots, \delta y_N)^T$,

$$\delta\mathbf{x} = \mathbf{Q}\delta\mathbf{y}. \tag{4}$$

For the case of slightly desynchronized system (the basic requirement for MSF analysis), the mode perturbations are growing with time as $\delta y_i(t) \propto \exp(\Lambda_i t)$, with $\Lambda_i, i = 1, \ldots, N$ the largest Lyapunov exponents calculated from Eq. (3). Since in Fig. 1 only the 2nd mode is slightly destabilized, while all other modes are still stable, we thus have $\delta y_2(t) \propto \exp(\Lambda_2 t)$, while $\delta y_l(t) \to 0$ for other modes. (For mode $l = 1$, the largest Lyapunov exponent is 0, which leads to the constant infinitesimal perturbation for δy_1.) Therefore, the mode perturbations can be treated as $(0, \delta y_2, \ldots, 0)^T$, based on which the Eq. (4) can be simplified to

$$\delta x_i = e_{2,i}\delta y_2, \tag{5}$$

where $\mathbf{e}_2 = (e_{2,1}, e_{2,2}, \ldots, e_{2,N})$ is the normalized eigenvector associated with λ_2 in the coupling matrix. For $\Lambda_2 \ll 1$, we have $\delta y_2 \propto \exp(\Lambda_2 t) \approx \Lambda_2 t$. Inputting this into Eq. (5), finally we get the following estimation for the trajectory perturbations

$$\delta x'_i \propto |e_{2,i}|. \tag{6}$$

This equation is the key to our identification of the unstable nodes, since it states that, statistically, the synchronization error of a node is *linearly proportional* to the eigenvector element that the node stands in the destabilized eigenmode.

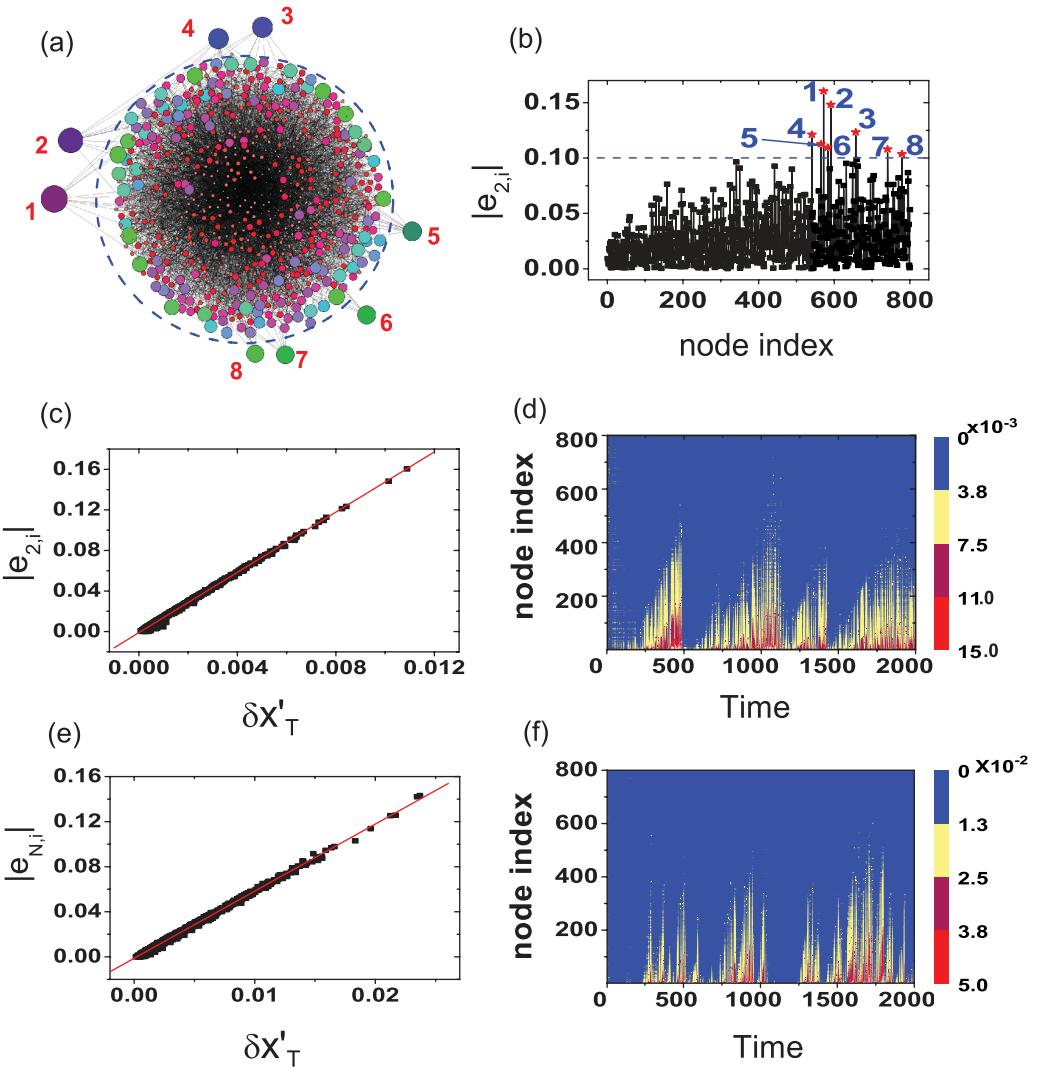

FIG. 2. (Color online) For the same network dynamics as plotted in Fig. 1 ($\varepsilon = 0.935$ and only the 2nd mode is slightly destabilized), (a) the replotted snapshot of the node synchronization errors, $\delta x'_i$, (b) the distribution of the eigenvector element for the destabilized mode, $\mathbf{e}_{2i}$, (c) the variation of the eigenvector element, $|e_{2,i}|$, as a function of the time-averaged synchronization error, $\delta x'_{iT}$, and (d) after reordering the network nodes, the time evolution of the synchronization errors. The 8 nodes which have the largest synchronization errors in (a) correspond to exactly the 8 nodes which have the largest eigenvector element in (b). By $\varepsilon = 1.05$ (only the Nth mode is slightly destabilized), (e) the variation of the eigenvector element, $|e_{N,i}|$, as a function of $\delta x'_{iT}$, and (f) the time evolution of the synchronization errors with the network nodes be reordered according to the amplitude of the eigenvector elements. For both (c) and (e), we have numerically the relationship $|e_i| \propto \delta x'_T$, which agrees with the theoretical predication of Eq. (6).

The correspondence between $\delta x'_i$ and $|e_{2,i}|$, as described by Eq. (6), is well justified by numerical simulations. In Fig. 2(a), we replot Fig. 1(a) by rearranging the nodes according to their synchronization errors, i.e., nodes of the largest (smallest) synchronization errors are arranged on the periphery (center) of the network. In particular, at the most outer-ring of the network, there locates the 8 most unstable nodes, which are ordered as $\delta x'_1 > \delta x'_2 > \cdots > \delta x'_8$. In Fig. 2(b), by the distribution of the eigenvector element, $|e_{2,i}|$, we also mark the 8 nodes which have the largest value of $|e_{2,i}|$. By checking the indices of the two set of nodes in the original network, it is found that the 8 unstable nodes observed in Fig. 2(a) are *exactly* matched with the 8 nodes marked in Fig. 2(b). For instance, the node of the largest synchronization error in Fig. 2(a), $\delta x'_{570} \approx 1.1 \times 10^{-2}$ is just the one owning the largest eigenvector element, $|e_{2,570}| \approx 0.16$, in Fig. 2(b).

As we have mentioned earlier, during the process of network evolution, the node synchronization errors [as plotted in Fig. 2(a)] will be dynamically changing with time. This makes it necessary to check whether the identification works for other moments of the evolution. Meanwhile, at the current stage it is still unknown whether the same method can be used to characterize the stability of the other nodes in the network. To answer these questions, we have checked numerically the statistical relationship between the eigenvector element, $|e_{2,i}|$ and the time-averaged synchronization error, $\delta x'_{iT}$, for all the network nodes. The results are plotted in Fig. 2(c). Here, it is clearly seen that, with the increase of $\delta x'_{iT}$, the value of

$|e_{2,i}|$ indeed is linearly increased, as predicted by Eq. (6). Our numerical results thus suggest that, besides the most unstable nodes, the stability of the other nodes in the network can still be well characterized by the proposed method.

Having revealed the linear relationship between the eigenvector, $|e_{2,i}|$, and the synchronization error, $\delta x_i'$, the identification of the synchronous patterns in complex networks is straightforward. Resorting the nodes by the decreasing order of the eigenvector elements, i.e., $|e_{2,1}| \geqslant |e_{2,2}| \geqslant \cdots \geqslant |e_{2,N}|$, in Fig. 2(d) we replot the time evolution of the synchronization errors presented in Fig. 1(b). It is found that, in contrast to the seemingly random dynamics [Fig. 1(b)], visible synchronous patterns are presented. More specifically, at any moment of the system evolution, the nodes of the smaller indices *always* have the larger synchronization errors, despite of the intermittent network dynamics. For this feature, we also say that the pattern are timely stable. Another feature of the pattern observed in Fig. 2(d) is that, during the episodes of network desynchronization (the "off" states), the synchronization errors are always propagated by a sequence of the reordered node index. For instance, during the period from $t = 300$ to 500, it is the node $i = 1$ (which corresponds to node 570 in the original index) that be firstly perturbed from the uniform synchronization background, and then this perturbation is gradually propagated to other nodes by the increasing order of the node index. In this sense, the patterns visualized in Fig. 2(d) not only reflect the distribution and evolution of the synchronization errors, but also showing the paths how the perturbations are propagated on the network. [This path of perturbation propagation, however, is virtual, and should not be understood as a real path composed by the directly connected nodes in the network. Say, for instance, if we use the most unstable node as the center and reordering the other nodes by their distances to it, we get the similar picture as Fig. 1(b), instead of the visible pattern as shown in Fig. 2(d).]

To check the application scope of the proposed method, we gradually decrease the coupling strength, so as to make the system be shifting to the deeply desynchronized regime. The simulations show that, around the transition point ε_1, as the coupling strength is decreased to 0.93 (below which the 3rd eigenmode becomes unstable), the linear relationship between $|e_{2,i}|$ and $\delta x_{iT}'$ are still well kept. However, by further decreasing the coupling strength, this linear relationship will be gradually destroyed, and the patterns becomes to be smeared. Finally, at about $\varepsilon = 0.72$ (below which the 4th eigenmode becomes unstable), there is no more clear relationship between $|e_{2,i}|$ and $\delta x_{iT}'$, and the patterns return to random again. So, nearby the transition point ε_1 the region for the clear node (pattern) identification is estimated to be $\varepsilon \in (0.93, \varepsilon_1)$.

The same identifications also work when the network is desynchronized from the other transition point, ε_2. In this case, it is the Nth eigenmode of the coupling matrix that be destabilized. As a result, the identification should be carried out based on the property of the eigenvector $\mathbf{e}_N$. To demonstrate this, we choose $\varepsilon = 1.05 > \varepsilon_2$, and re-simulate the evolution of the system dynamics. Similar to the results in Fig. 1, the system is also found to be undergoing the process of intermittent synchronization, and the synchronization errors for a few of the nodes are distinguishingly large. In Fig. 2(e), we plot the eigenvector element, $|e_{N,i}|$, as a function of the node synchronization error, $\delta x_{iT}'$. Just like the case of mode 2 be destabilized, a linear relationship is also observed between $|e_{N,i}|$ and $\delta x_{iT}'$. Reordering the nodes according to $|e_{N,i}|$, we plot in Fig. 2(f) the time evolution of the synchronization errors, which, again, shows the visible synchronous patterns.

Besides the situation of one-mode be destabilized, the unstable nodes and synchronous patterns can still be well identified even when the 2nd and Nth eigenmodes are (slightly) destabilized simultaneously. This has been verified by another scale-free-type network, which is specially constructed so as to make both two boundary eigenmodes be slightly outside of the stable regime. In this 2-mode destabilized case, we find that it is the eigenmode which has the larger value of Λ that governs the identification. More specifically, if $\Lambda_2 > \Lambda_N$ ($\Lambda_2 < \Lambda_N$), the network nodes should be reordered by the decreasing order of the element for the eigenvector $\mathbf{e}_2$ ($\mathbf{e}_N$).

IV. PATTERN IDENTIFICATION IN CLUSTERED COMPLEX NETWORKS

It has been well known that the dynamics of a complex network could be largely affected by its underlying topology [5], which makes it necessary to check the validity of our method of node (patten) identification for other types of network models besides the scale-free-type networks. To this end, we have checked the same identifications for three other types of complex networks that have been widely investigated in literature, including the random networks, the small-world networks, and the clustered networks [32]. For the random and small-world networks, it is shown that, given the network is slightly desynchronized, the unstable nodes can always be properly identified by the method of eigenvector analysis, as well as the synchronous patterns (not shown). However, when dealing the clustered networks, it is found that the current method is no more effective. Specifically, we find that the current method can only identify the unstable nodes (synchronous patterns) within each cluster, but failing to do this for the whole network. This finding thus suggests that, to analyze the clustered networks, the current method should be improved.

A distinguishing feature of the clustered network is that the probability for a pair nodes to be connected inside a cluster is much higher than that of different clusters [32]. As far as the network eigenvectors are concerned, a significant change caused by this topological feature is that the elements of the 2nd eigenvector are of stage-like distribution [33,34]. That is, for a m-cluster network, the elements of the 2nd eigenvector are clearly divided into m groups, with each group stays on an individual platform. Since our method of node (pattern) identifications is established on the eigenvectors of the destabilized modes, the stage-like property of the 2nd eigenvector thus is crucial to the proper identification of the unstable nodes and synchronous patterns. Now the question is: how to use the stage-like property of the 2nd eigenvector in clustered complex networks for the purpose of node (pattern) identification?

To investigate, we first consider the simple case of 2-cluster complex network. The size of the 1st cluster is $N_1 = 120$, and the 2nd one is $N_2 = 80$. Meanwhile, to make the cluster feature clear, nodes inside each cluster are connected by a larger

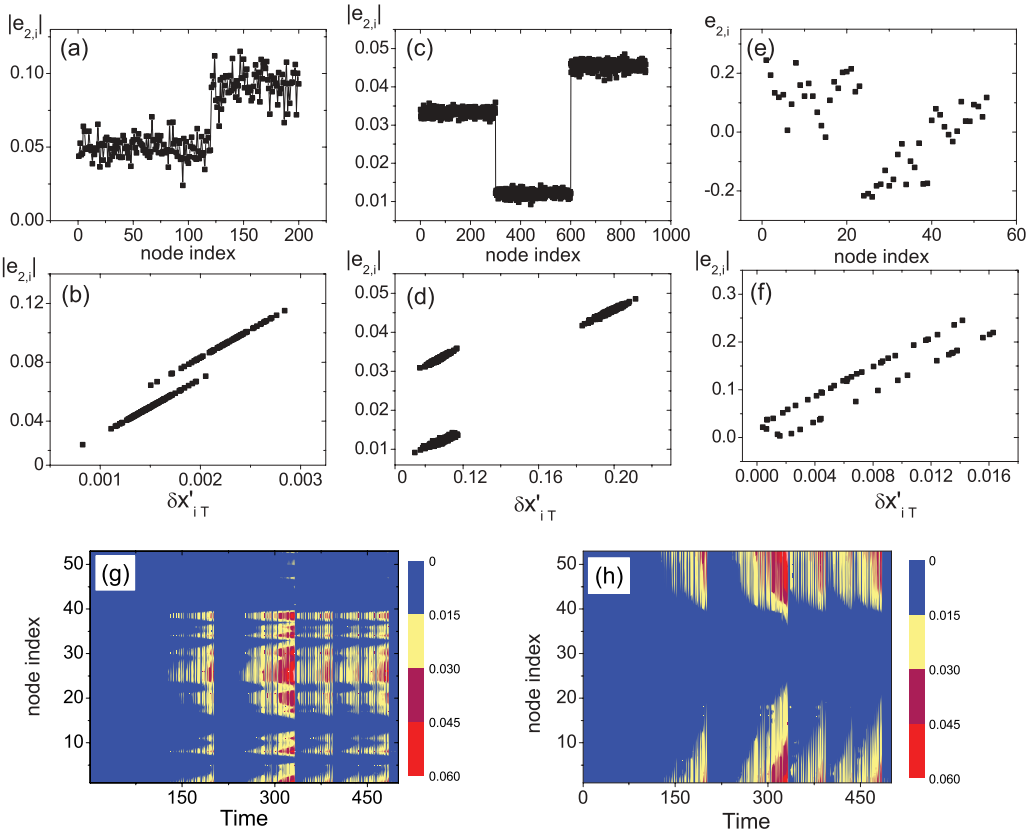

FIG. 3. (Color online) The eigenvector of the 2nd eigenmode and the relationship between the eigenvector element, $|e_{2,i}|$ and the node synchronization error, $\delta x'_{iT}$, for a 2-cluster network [(a),(b)], a 3-cluster network [(c),(d)], and the cat-brain network [(e),(f)]. (g) For the slightly desynchronized cat-brain network, the evolution of the system dynamics with the original node index. (h) The evolution of the system dynamics with the node index be reordered according to the improved method.

probability, $p_i = 0.8$, while nodes in different clusters are connected by a much smaller probability, $p_l = 0.1$. In Fig. 3(a), we plot the distribution of $|e_{2,i}|$ for the 2nd eigenmode. It is seen clearly that the elements are divided into two groups, while each group stands for a cluster. By tuning the coupling strength, we let the network be slightly desynchronized from the transition point ε_1. The relationship between the eigenvector element, $|e_{2,i}|$, and the node synchronization error, $\delta x'_{iT}$ is plotted in Fig. 3(b). It is found that, different from the scale-free-type networks, the relationship between $|e_{2,i}|$ and $\delta x'_{iT}$ is decomposed to two linear branches. Also, a checking of the node index shows that each branch just corresponds to one cluster in the network.

The brunched correspondence between $|e_{2,i}|$ and $\delta x'_{iT}$ is common for the clustered complex networks. In Figs. 3(c) and 3(d), we do the same analysis for a 3-cluster complex network, where the size of the clusters is identical, $N_1 = N_2 = N_3 = 300$. Again, it is observed that the eigenvector elements are divided into 3 groups, and the relationship between $|e_{2,i}|$ and $\delta x'_{iT}$ consists of 3 linear branches. Also, the eigenvector elements [Fig. 3(c)] and the brunches [Fig. 3(d)] are organized according to the network clusters.

The finding that in a m-cluster network the correspondence between $|e_{2,i}|$ and $\delta x'_{iT}$ is decomposed into m branches seems to suggest the following method for nodes (pattern) identification: *regrouping nodes according to the clusters, and then reordering the nodes within each cluster according to their eigenvector elements*. To verify this improved method, we have analyzed the identifications of the unstable nodes and patterns in the desynchronized cat-brain network. The cortico-cortical network of cat brain consists of 53 nodes (cortex areas) and about 830 links (fiber connections) [35]. The cluster features, as well as other properties of this network, has been well investigated in previous studies [36,37]. According to their functions, the cortex areas are roughly divided into two major divisions: the visual and auditory division which contains 23 areas, and the somatomotor and frontolimbic division which contains 30 areas.

To facilitate the analysis, we neglect the details of the link weights in the original system, while adopting the general scheme of weighted gradient network to investigate the synchronization problem [23]. Under this scheme, the coupling matrix in Eq. (1) is replaced by $c_{ij} = a_{ij}k_j^\beta / \sum_j (a_{ij}k_j^\beta)$, with β a parameter that characterizes the distribution of the link weight. An advantage of this coupling scheme is that the network synchronizability can be flexibly adjusted without changing the network structure. Setting $\beta = 0.5$, the two boundary eigenvalues are $\lambda_2 = -0.47$ and $\lambda_N = -1.29$. With $\varepsilon = 1.04$ (which is slightly below the transition point ε_1), the 2nd eigenmode becomes unstable, with $\Lambda_2 \approx 0.02$. The seemingly random evolution of the node synchronization errors are plotted in Fig. 3(g), where the phenomenon of

intermittent synchronization is evident. Regrouping nodes into two clusters [Fig. 3(e)] and reordering nodes inside each cluster according to their eigenvector elements [Fig. 3(f)], it is found that the synchronization errors indeed can be regulated to visible patterns, as shown in Fig. 3(h). It is interesting to see that, corresponding to the clusters, the patterns are clearly decomposed into two bands. [In Fig. 3(h), to guide the eyes, nodes in the first cluster is reordered by an increasing order of the eigenvector element.]

As the improved method is based on the stage-like distribution of the eigenvector, it is natural that, given the network has the clear cluster structure (whatever the size distribution of the clusters), the improved method should be always workable. However, if the cluster feature is not clearly presented in the network, e.g., $p_i \approx p_l$, this method will lost it efficiency, and should be replaced by the original method (the one discussed in Sec. III).

V. DISCUSSIONS AND CONCLUSION

So far our studies have been focused on the only simple case of coupled identical logistic maps. Since realistic networks are typically represented by the coupled non-identical time-continuous oscillators, it is therefore necessary to check whether the identification method can be also applied to the general complex systems. To check this out, we replace the node dynamics with the chaotic Rössler oscillators which, in its isolated form, is described by $\mathbf{F}_i(\mathbf{x}_i) = [-\omega_i y_i - z_i, \omega_i x_i + 0.2 y_i, 0.2 + (x_i - 5.7) z_i]$, with $\mathbf{x} = (x, y, z)$ and ω_i is the natural frequency of the oscillator. The coupling function is chosen as $\mathbf{H}(\mathbf{x}) = x$, with which the stable regime of the MSF curve is bounded. This time, we generate a scale-free-type network of $N = 100$ nodes with the average degree $\langle k \rangle = 8$. By the gradient coupling scheme ($\beta = 0.5$), the two boundary eigenvalues of the network are $\lambda_2 = -0.5$ and $\lambda_N = -1.6$. In the case of identical oscillators, i.e., $\omega_i = \omega = 1$, from the MSF analysis we can obtain the range of coupling strength for network synchronization, which is $\varepsilon \in (0.31, 2.82)$. To make the oscillators nonidentical, we randomly choose 5 of the oscillators in the network and change their natural frequency to $\omega_j = \omega' = 0.995$. (This model of nonidentical network is somewhat artificial, but could be still constructive to the identification of synchronous pattern in some non-identical networks, e.g., a slightly variation of the natural frequency among the Rössler oscillators. However, when the node dynamics are of significant difference, e.g., a large variation of the oscillator parameters or the node dynamics has different types, it remains a challenge how to identify the synchronous patterns properly.)

With $\varepsilon = 0.29$, the network is slightly desynchronized from the transition point $\varepsilon_1 \approx 0.31$, and showing the phenomenon of intermittent network synchronization, as depicted in Fig. 4(a). It is noticed that, comparing to the majority oscillators which has the parameter $\omega = 1$, the 5 oscillators of the parameter $\omega' = 0.995$ are much more unstable. The large synchronization errors of the 5 nodes can be attributed to the following two reasons. Firstly, due to the parameter mismatch, the transition point for oscillators of ω' is larger to that of ω, i.e., $\varepsilon_1(\omega') > \varepsilon_1(\omega)$, which leads to $\Lambda_2(\omega') > \Lambda_2(\omega)$ and consequently the larger synchronization errors for these 5 oscillators. Secondly,

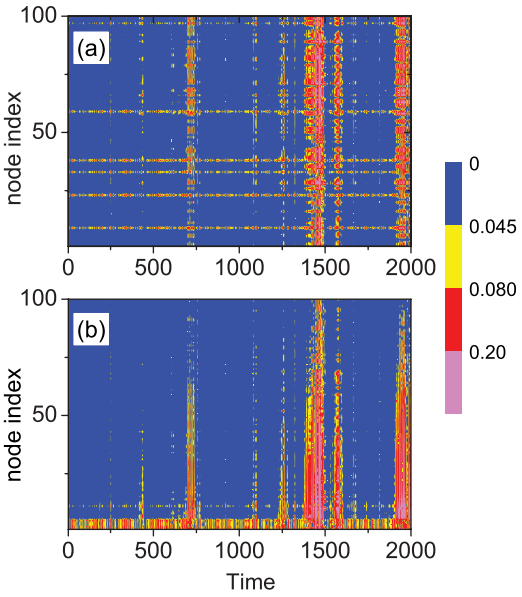

FIG. 4. (Color online) For the network of non-identical chaotic Rössler oscillators, the time evolution of the node synchronization errors with (a) the original node index and (b) the reordered node index. In (a), the 5 (interrupted) horizontal lines occur at the nodes of the differentiated parameter, ω'. In plotting (b), the 5 nodes of the parameter ω' are given the smallest indices, 1 to 5, while the resting nodes are reordered according to the eigenvector element, $|e_{2,i}|$, as did in Figs. 2 and 3.

since the node synchronization error is defined as the difference to the network-averaged state, i.e. $\delta x_i' = |x_i - \bar{x}|$, it is natural that the minor nodes of the different parameter will have larger synchronization errors. Having understood these, it is straightforward to improve the identification method as follows: treating the minor nodes of the different parameter specially (giving the smallest indices), and then reordering the other nodes of the network by the eigenvector element as before. This improved method indeed works well, as depicted in Fig. 4(b).

To test the generality of the findings, we have carried extensive simulations on a variety of network models, including adopting different types of MSF curves, using different coupling schemes, as well as considering other types of dynamics for the oscillators. All the results show that, given the network is slightly desynchronized, the unstable nodes and the synchronous patterns can always be properly identified by the method of eigenvector analysis. Although in the present work we regard the phenomenon of intermittent synchronization as the mark of "slight synchronization", it should be pointed out that the application of the method is not limited to this special phenomenon. In our simulations, it is noticed that in some special situations, even the network is not slightly desynchronized, the unstable nodes and synchronous patterns can still be identified. For instance, under the scheme of gradient coupling, the unstable nodes (patterns) in the network of Fig. 1 can be identified reasonably well even a number of the eigenmodes (up to 20 eigenmodes) are destabilized simultaneously. Another thing worthy of mentioning is that the identifications are robust to the noise perturbations. For instance, when iid random noise of strength 1×10^{-2} is added to the network of chaotic Rösslers used in Fig. 4 during the

system evolution, the synchronous patterns are still clearly presented.

In summary, by the method of eigenvector analysis, we have investigated the identifications of the unstable nodes and synchronous patterns in slightly desynchronized complex networks. It is found that, despite of the complex network structure and the complicated network dynamics, the synchronization stability of the individual nodes can still be well predicted and characterized. Moreover, with this identification method, the seemingly random dynamics of the desynchronized networks can be regulated into stable and visible synchronous patterns. We have tested this method for a variety of network models and for different desynchronization schemes, where the general finding is that, given the network is slightly desynchronized, the unstable nodes and synchronous patterns can always be effectively identified. Considering the universal existence of synchronization in nature and the close relationship between the synchronization behavior and the system functions, it is our believing that the findings obtained will be helpful to the exploration of the high-level functions in broad realistic systems, say, for instance, the generation of consciousness and mind in the network of human brain [38].

ACKNOWLEDGMENTS

XGW acknowledges sponsorship from the Scientific Research Foundation for the Returned Overseas Chinese Scholars, State Education Ministry. This work was also supported by the National Natural Science Foundation of China under Grants No. 10805038 and No. 10975117.

[1] A. M. Turing, Philos. Trans. R. Soc. London B **237**, 37 (1952).
[2] M. C. Cross and H. Greenside, *Pattern Formation and Dynamics in Nonequilibrium Systems*, (Cambridge University Press, Cambridge, 2009).
[3] V. Castets, E. Dulos, J. Boissonade, and P. De Kepper, Phys. Rev. Lett. **64**, 2953 (1990).
[4] Q. Ouyang and H. L. Swinney, Nature (London) **352**, 610 (1991).
[5] D. J. Watts and S. H. Strogatz, Nature (London) **393**, 440 (1998).
[6] A.-L. Barabási and R. Albert, Science **286**, 509 (1999).
[7] R. Albert and A.-L. Barabási, Rev. Mod. Phys. **74**, 47 (2002).
[8] K. Park, L. Huang, and Y.-C. Lai, Phys. Rev. E **75**, 026211 (2007).
[9] J. P. Crutchfield, Nat. Phys. **8**, 17 (2012).
[10] H. Nakao and A. S. Mikhailov, Nat. Phys. **6**, 544 (2010).
[11] Y. Qian, X. Huang, G. Hu, and X. Liao, Phys. Rev. E **81**, 036101 (2010).
[12] X. Liao, Q. Xia, Y. Qian, L. Zhang, G. Hu, and Y. Mi, Phys. Rev. E **83**, 056204 (2011).
[13] M. V. Sanchev-Vives and D. A. McCormick, Nat. Neurosc. **3**, 1027 (2000).
[14] Y. Kuramoto, *Chemical Oscillations, Waves and Turbulence* (Springer-Verlag, Berlin, 1984).
[15] A. S. Pikovsky, M. G. Rosenblum, and J. Kurths, *Synchronization: A Universal Concept in Nonlinear Science* (Cambridge University Press, Cambridge, UK, 2001).
[16] S. Boccaletti, V. Latora, Y. Moreno, M. Chavez, and D.-U. Hwang, Phys. Rep. **424**, 175 (2006).
[17] A. Arenas, A. Diaz-Guilera, J. Kurths, Y. Moreno, and C. Zhou, Phys. Rep. **469**, 93 (2008).
[18] X. F. Wang and G. Chen, Int. J. Bifurcation Chaos Appl. Sci. Eng. **12**, 187 (2002); T. Nishikawa, A. E. Motter, Y.-C. Lai, and F. C. Hoppensteadt, Phys. Rev. Lett. **91**, 014101 (2003); D.-U. Hwang, M. Chavez, A. Amann, and S. Boccaletti, *ibid.* **94**, 138701 (2005); C. Zhou, A. E. Motter, and J. Kurths, *ibid.* **96**, 034101 (2006).
[19] A. E. Motter, C. Zhou, and J. Kurths, Europhys. Lett. **69**, 334 (2005); Phys. Rev. E **71**, 016116 (2005); AIP Conf. Proc. **778**, 201 (2005).
[20] X. G. Wang, S. Guan, Y.-C. Lai, B. Li, and C.-H. Lai, Europhys. Lett. **88**, 28001 (2009).
[21] X. G. Wang, Eur. Phys. J. B **75**, 285 (2010).
[22] J. Altenburg, R. J. Vermeulen, R. L. M. Strijers, W. R. Fetter, and C. J. Stam, Clinical Neurophysiol. **114**, 50 (2003).
[23] X. G. Wang, Y.-C. Lai, and C. H. Lai, Phys. Rev. E **75**, 056205 (2007).
[24] L. M. Pecora and T. L. Carroll, Phys. Rev. Lett. **80**, 2109 (1998).
[25] G. Hu, J. Z. Yang, and W. Liu, Phys. Rev. E **58**, 4440 (1998).
[26] M. Barahona and L. M. Pecora, Phys. Rev. Lett. **89**, 054101 (2002).
[27] L. Huang, Q. Chen, Y.-C. Lai, and L. M. Pecora, Phys. Rev. E **80**, 036204 (2009).
[28] L. A. Bunimovich, A. Lambert, and R. Lima, J. Stat. Phys. **65**, 253 (1990); J. F. Heagy, T. L. Carroll, and L. M. Pecora, Phys. Rev. Lett. **73**, 3528 (1994); J. F. Heagy, L. M. Pecora, and T. L. Carroll, *ibid.* **74**, 4185 (1995).
[29] M. A. Matias, V. Perez-Munuzuri, M. N. Lorenzo, I. P. Marino, and V. Perez-Villar, Phys. Rev. Lett. **78**, 219 (1997); G. Hu, J. Yang, and W. Liu, Phys. Rev. E **58**, 4440 (1998).
[30] H. Fujisaka and T. Yamada, Prog. Theor. Phys. **84**, 918 (1985); H. Fujisaka, H. Ishii, M. Inoue, and T. Yamada, *ibid.* **76**, 1198 (1986).
[31] N. Platt, E. A. Spiegel, and C. Tresser, Phys. Rev. Lett. **70**, 279 (1993); E. Ott and J. C. Sommerer, Phys. Lett. A **188**, 39 (1994); Y. Nagai and Y.-C. Lai, Phys. Rev. E **55**, 1251 (1997).
[32] M. E. J. Newman, SIAM Rev. **45**, 167 (2003).
[33] L. Huang, K. Park, Y. C. Lai, L. Yang, and K. Yang, Phys. Rev. Lett. **97**, 164101 (2006).
[34] X. G. Wang, L. Huang, Y.-C. Lai, and C. H. Lai, Phys. Rev. E **76**, 056113 (2007).
[35] J. W. Scannell, G. A. P. C. Burns, C. C. Hilgetag, M. A. O'Neil1, and M. P. Young, Cereb. Cortex **9**, 277 (1999).
[36] O. Sporns and J. D. Zwi, Neuroinformatics **2**, 145 (2004).
[37] C. Zhou, L. Zemanova, G. Zamora, C. C. Hilgetag, and J. Kurths, Phys. Rev. Lett. **97**, 238103 (2006).
[38] O. Sporns, D. R. Chialvo, M. Kaiser, and C. C. Hilgetag, Trends Cogn. Sci. **8**, 418 (2004).